Stable Unimanual and Bimanual Manipulation of a Power Drill

Nicolas Aarons
Department of Mechanical Engineering, MIT
Cambridge, MA 02139
nicarons@mit.edu

James Hermus
Department of Mechanical Engineering, MIT
Cambridge, MA 02139
jhermus@mit.edu

Abstract— **Humans easily bimanually manipulate objects which may induce contact or coupled instability. The task of using a power drill is especially interesting as instability may arise in several ways. In this work we explore the task of power drilling with one and two Kuka Iiwa arms through simulation in drake. The task was accomplished by super imposing several controllers: an impedance to regulate gripper translation and rotation, a nullspace projected joint space impedance to resolve the redundancy, a feedforward torque to compensate the mass of the drill after it was picked up, and a torque to compensate for gravity. Impedances were chosen to be human-like. Minimum jerk trajectories smoothly moved the nominal position of the gripper controller between waypoints. The second Iiwa, when used, provided a stabilizing impedance in all directions except for downwards to not interfere with the task. Using this approach, both the unimanual and bimanual systems were able to move into stable contact with the ground and generate a downward force on the drill of 32 Newtons.**

Keywords— Impedance, Bimanual Manipulation, Contact Stability

I. Introduction

A. Contact and Couple Stability

Humans are incredibly dexterous and excel at physical interaction with complex objects, despite large feedback delays and many degrees of freedom. An interesting example of such a manipulation task is the bimanual manipulation of a power drill. Using a power drill is especially thought-provoking as instability may arise in several ways[1]: pushing on the drill generates destabilizing torques, grasping the drill with both hands creates a closed kinematics chain which can induce coupled instability, and the drill generates destabilizing torques of its own as it rotates. These stability concerns motivate the consideration of energetically passive controllers [2], [3].

B. Dynamic Primatives

To accomplish such astonishing performance, we hypothesize that human motor behavior, with and without physical interaction, is constructed using a limited set of primitive dynamic behaviors, including oscillations, submovements, and mechanical impedances [4], [5]. We propose that not only these dynamic primitives exist but also that they are connected by a Norton equivalent network (Figure 1) [6].

Mounting evidence suggests that these structures are not simply emergent patterns but limitations on human control. These primitives may make control planning easier for several reasons. First, they provide a small parameter space to search. Second, even complex and nonlinear mechanical impedances superimpose linearly. Finally, this type of control easily scales to many degrees of freedom.

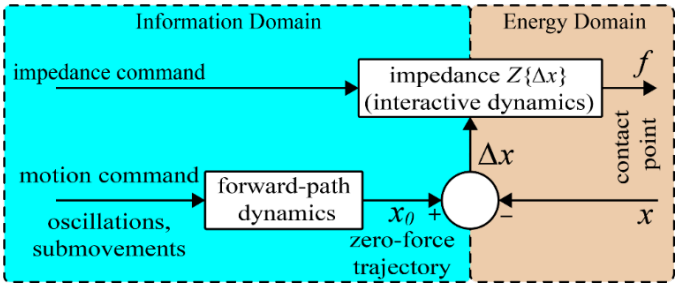

Figure 1: A nonlinear equivalent network relating the information and energy domains of dynamic behavior. Motion primitives determined by central commands comprise the forward path to produce a zero-force trajectory. Impedance, also determined by central commands, relates the zero-force trajectory, motion, and force to produce the contact point behavior.

In this project, we developed a simulation and control where two kuka LBR iiwa arms grasp a power drill. One iiwa supported the drill while the other will apply a downward force to the drill. While this task involves bimanual manipulation and unstable contact, it was relatively simple to accomplish given a controller composed of dynamic primitives.

II. Methods

This section will present the control and simulation methods for the work. In this section several subcomponents of the project will be described: the iiwa controller, the gripper control, the waypoint control, the state machine, the software architecture, and the model of the power drill.

A. Arm Torque Control

The simulations in this work were performed in DRAKE using a model of the seven degree of freedom torque-controlled KUKA LBR iiwa R800 (LBR).

The analytical Jacobian matrix $J(q) \in \mathbb{R}^{6\times n}$ of the robot was denoted by:

$$\boldsymbol{J}(q) = \begin{bmatrix} J(q)_x \\ J(q)_\theta \end{bmatrix} \tag{1}$$

Here, $\boldsymbol{J}(\boldsymbol{q})_x \in \mathbb{R}^{3\times n}$ maps the joint velocities $\dot{\boldsymbol{q}} \in \mathbb{R}^n$ to translational end-effector velocities and $\boldsymbol{J}(\boldsymbol{q})_\theta \in \mathbb{R}^{3\times n}$ maps $\dot{\boldsymbol{q}}$ to rotational gripper velocities. In order to define the controller,

three rotational reference frames were defined: a fixed world frame denoted Σ_W, a moving frame fixed to gripper, denoted Σ_G, and a frame moving with the LBR robot's zero-force trajectory, denoted Σ_0. Both, $\boldsymbol{J}(\boldsymbol{q})_x$ and $\boldsymbol{J}(\boldsymbol{q})_\theta$ were expressed with respect to the gripper frame. For the gripper translational impedance controller, the desired control torque $\boldsymbol{\tau_x} \in \mathbb{R}^n$ was computed by:

$$\boldsymbol{\tau_x} = \boldsymbol{J_x^T}(\boldsymbol{K}_x(\boldsymbol{x}_0 - \boldsymbol{x}) + \boldsymbol{B}_x(-\dot{\boldsymbol{x}})) \quad (2)$$

This torque described a translational spring-damper system with linear stiffness $\boldsymbol{K}_x \in \mathbb{R}^{3\times3}$ and linear damping $\boldsymbol{B}_x \in \mathbb{R}^{3\times3}$. Both $\boldsymbol{K}_x$ and $\boldsymbol{B}_x$ were chosen to be diagonal matrices. The virtual spring was attached between the Σ_G and Σ_0 frame. The position of the gripper $\boldsymbol{x} \in \mathbb{R}^3$ and the zero-force position $\boldsymbol{x}_0 \in \mathbb{R}^3$ were represented in the base frame coordinates Σ_W. The zero force trajectory, $\boldsymbol{x}_0$, was regulated through waypoints using minimum jerk trajectories described in a later section. For the gripper rotational impedance controller, the desired control torque $\boldsymbol{\tau_x} \in \mathbb{R}^n$ was computed by:

$$\boldsymbol{\tau_\theta} = \boldsymbol{J_\theta^T}(\boldsymbol{K}_\theta(\hat{u}_0\theta_0) + \boldsymbol{B}_\theta(-\dot{\boldsymbol{\theta}})) \quad (3)$$

The rotational torque $\boldsymbol{\tau_\theta}$ aligned the axes of frame Σ_G and moving frame Σ_0. The rotation between Σ_G and Σ_0 was expressed by the rotation matrix ${}^0R_e \in SO(3)$. To calculate the rotational torque $\boldsymbol{\tau}_\theta$, ${}^0R_e$ was converted to axis-angle representation, with unit axis $\hat{\boldsymbol{u}}_0 \in \mathbb{R}^3$ and angle $\boldsymbol{\theta}_0 \in \mathbb{R}^3$ [7], [8]. Thus, a virtual rotational spring with rotational stiffness $\boldsymbol{K}_\theta \in \mathbb{R}^{3\times3}$ was attached around $\hat{u}_0$ to rotate about θ_0. The rotational velocity $\dot{\boldsymbol{\theta}}_0 \in \mathbb{R}^3$ was damped with dissipating element $\boldsymbol{B}_\theta \in \mathbb{R}^{3\times3}$. Then, the translational and rotational gripper torques were combined,

$$\boldsymbol{\tau}_g = \boldsymbol{\tau}_x + \boldsymbol{\tau}_\theta \quad (4)$$

For the joint-space impedance controller, the commanded torque $\boldsymbol{\tau}_q \in \mathbb{R}^n$ was expressed by

$$\boldsymbol{\tau_q} = \boldsymbol{K}_q(\boldsymbol{q}_0 - \boldsymbol{q}) + \boldsymbol{B}_q(-\dot{\boldsymbol{q}}) \quad (5)$$

with joint-space stiffness $\boldsymbol{K}_q \in \mathbb{R}^{n\times n}$ and joint-space damping $\boldsymbol{B}_q \in \mathbb{R}^{n\times n}$. The nominal joint position $\boldsymbol{q}_0 \in \mathbb{R}^n$ was constant throughout the simulations. A nullspace projector $N \in \mathbb{R}^{n\times n}$ was computed by

$$\boldsymbol{N} = \boldsymbol{I} - \boldsymbol{J}(\boldsymbol{q})^T\left(\boldsymbol{J}(\boldsymbol{q})^{\#}\right)^T \quad (6)$$

Multiplying the torque resulting from the joint space stiffness ensured that the joint torque did not conflict with the gripper task [9], [10]. We acknowledge that the Moore Penrose pseudo inverse used in this work does not ensure passivity. This is a limitation of the current implementation and will be addressed in the discussion.

A feedforward torque τ_{ff} was added to compensate for the weight of the drill after it was picked up. A torque $\boldsymbol{\tau}_G$ compensated for the influence of gravity on the robot its self.

Superimposing these torque controllers, the command send to the actuators was achieved.

$$\boldsymbol{\tau}_{act} = \boldsymbol{\tau}_g + \boldsymbol{N}\boldsymbol{\tau}_q + \boldsymbol{\tau}_{ff} + \boldsymbol{\tau}_G \quad (7)$$

In practice, the parameters of the controller used during contact are displayed below.

Variable	Values	Units
K_x	Diag([2000,2000,2000])	N/m
B_x	$0.2K_x$	N-s/m
K_θ	Diag([100,100,10])	N-m/rad
B_θ	Diag([40,40,40])	N-m-s/rad
K_q	Diag([20,20,20, 20,20,20,20])	N-m/rad
B_q	$0.2K_q$	N-m-s/rad

B. Perturbation

In some of our simulations a sinusoidal 3, 10, or 30 Hz force perturbation with an amplitude of 10N was added to the gripper control of the first iiwa during the pushing task. The goal of adding this perturbation was to represent the forces which could be produced by the drill. This was a reasonable assumption because the drill did not slip from the gripper during the pushing task.

C. Gripper control

Both grippers had a similar control scheme with essentially two options, “closed” or “open”. For open, the grippers were commanded to a nominal position of [-0.05, 0.05] with a stiffness between the nominal and actual position of 2000N/m. For the closed position, the control of the grippers was somewhat more complex. The same approach as the open position, simple proportional position control, wouldn’t work the same for both grippers due to them grabbing onto parts of different thickness. Instead of making the gripping force thickness dependent, a constant 150N total gripping force was assigned. This, however, caused the object to move about relative to the robot as the drill was rotated as the gripper fingers had no nominal position. A stiffness was then added between the average of the fingers and the center of the gripper. This stiffness was made very high so that the gripper would consistently grip with 150N force and hold the drill approximately in the center of the gripper each time it grabs onto the drill.

D. Moving Smoothly Between Waypoints

Human movements are typically smooth and sterotyped. Research has shown that a nominal trajectory composed of minimum jerk profiles can well describe the obsered point to point movements of humans [11], [12]. For this reason, we determined waypoints and moved between them with a minimum jerk trajectory. This is a smooth bell shaped velocity profile described by a start postion, an amplitude, A, and a duration, D,

$$\boldsymbol{x(t)} = A\left(\frac{10}{D^3}\,t^3 - \frac{15}{D^4}t^4 + \left(\frac{6}{D^5}\right)t^5\right). \qquad (8)$$

This approach greatly decreased the amount of information required to control the robot, as far fewer parameters had to be chosen to move between waypoints. In addition, the smoothness allowed for much lower stiffness values to be achieved.

E. State Machine

The task was broken down into actions. An action was a programed event which would transition the robot from one state to the next. After an action was completed, a check was run to ensure each iiwa and the drill were within an acceptable range from the expected position. Figure 2 depicts the way in which the task was broken down in to actions. Other than the position the drill was moved to before the start of drilling, and the drilling location, all other positions were relative to the start or to the drill its self. This programing made the controller generalizable to different starting positions of the drill or target.

Unfortunately, our video examples do not show this structure because there were no unexpected collisions or failures. However, this structure should make it possible to add task planning on top of the existing design in the future.

F. Software Architecture

1) Inverse dynamics controller for gravity comp

We used Drake's built-in Inverse Dynamics Controller for gravity compensation of the iiwas. By setting the PID gains of the position control part of the Inverse Dynamics Controllers to 0, we were able to define our own torque controllers without having to worry about gravity compensation.

2) Iiwa torque controller variable impedance control

We defined our own torque controllers in drake as a subclass of Drake's LeafSystem with inputs of desired position for the gripper and joint configuration, the actual positions of the joints and gripper, and impedances and feedforward torques and forces specified from our state machine. We then calculated torques according the part A. Even though we are essentially doing position control of the gripper, making our own torque controller was useful for our project allowing us to change the impedance of the iiwas throughout a task, which the Inverse Dynamic Controller isn't capable of.

Summing the torque controller output and the gravity compensation gives the total torque outputted at the joints of each iiwa.

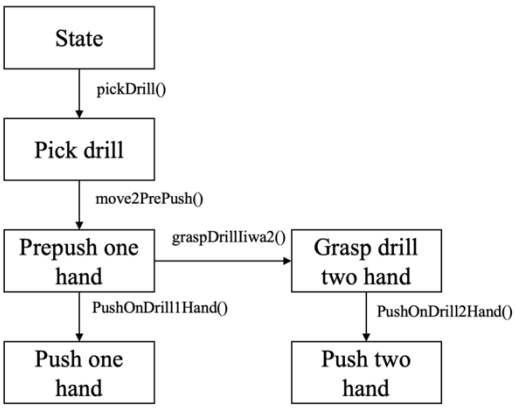

Figure 2: Diagram of state machine used to determine which actions should be run and if they have been achieved.

G. Drill Model

We used the same drill mesh model discussed in class as part of Label Fusion [13], it is currently available at (http://labelfusion.csail.mit.edu/data/LabelFusion_Sample_Data.tar). We used it in a sdf file by approximating the inertial properties. We found that using the visual mesh as collision geometry slowed down our simulation drastically and also resulted in much harder grasping for our iiwas. To combat this, we used a simplified model of the collision geometry for the drill. Figure 3 shows the visual mesh, the collision geometry and the two overlayed on top of each other.

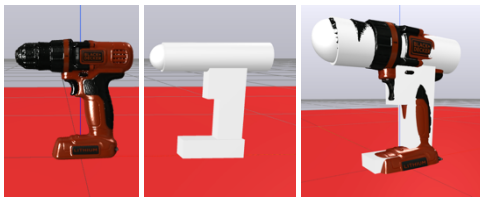

Figure 3: (left) Visual model of the drill used in simulation (middle) contact model of the drill used in simulation (right) overlayed contact model and visual model.

III. Results

A. One arm case

For the one arm, or unimanual, case, we initially ran in to some problems related to stability. After we picked up the drill and turned it our arm would oscillate exponentially, eventually throwing the drill away. We found that by reducing the rotational stiffness in the Z direction we were able to almost completely reduce this unstable oscillation. We think it was caused by our time step being too large.

After fixing this issue, we successfully completed the task, pushing down on the drill with a 32N force to simulate the act of drilling. This is shown in figure 5 below. The iiwa arm had some significant swaying or oscillation while in contact with the ground, pushing down on the drill, but it seemed to be still stable. The drill's orientation while drilling deviated from an upright posture, almost certainly because we didn't input a

feedforward torque to counteract the torque coming from the ground reaction force. Although unideal, this allowed us to see the improvements on drill orientation that the bimanual case had.

The iiwa was also successful in picking up and using the drill from many different drill starting locations and many different nominal joint configurations.

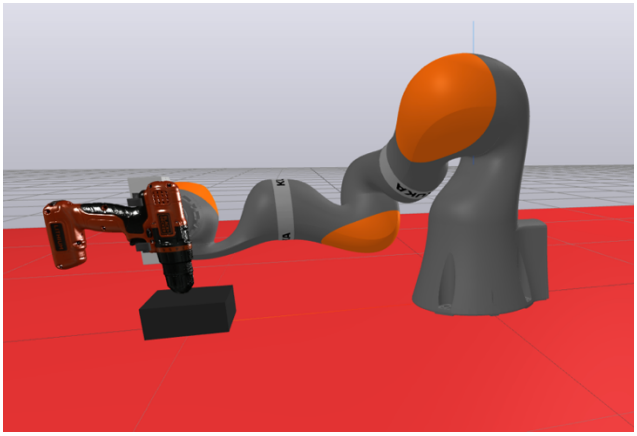

Figure 4: Stable unimanual manipulation of the drill during contact.

B. *Two arm case*

For the bimanual case, the first iiwa used the same control scheme as before. The second iiwa came in to play after the drill had been picked up and rotated. It then grabbed on to the drill as well.

After the second iiwa grabbed the drill, the Z translational impedance of it was set to zero. This ensured that the second iiwa didn't interfere with the drilling task but allowed it to provide added stability. Figure 6 shows the two iiwas working together to accomplish the task.

We saw much less swaying in the bimanual case as opposed to the unimanual case. We also saw a more upright drilling posture.

Unfortunately, due to time constraints and our limited knowledge of drake, we are unable to provide evidence of the reduced swaying and change in drilling posture past the videos linked in this paper. We hope to learn to export measurements of force and drill orientation in future simulations.

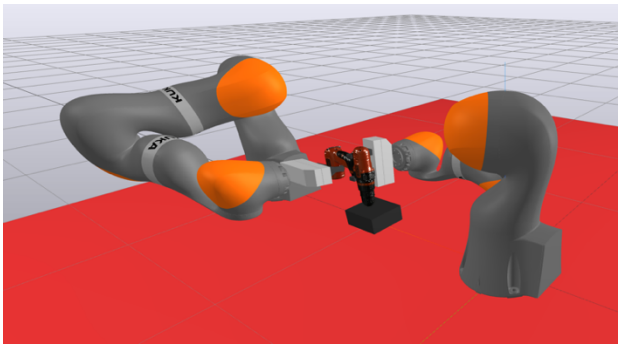

Figure 5: Stable bimanual manipulation of the drill during contact.

C. *Perturbation*

In the simulation with the 10N sinusoidal perturbations the task remained stable in both the unimanual and bimanual case. This suggests that while our control was robust, we may be able to decrease the impedance of the robot and still be stable and achieve the task.

IV. Discussion

This was our first time working within a simulation framework to accomplish a manipulation task. We now have a far better understanding of the DRAKE simulation environment. Furthermore, with a broader understanding of the field of manipulation as a whole, we hope to investigate the use of optimization to develop a small library of actions which can learn robot nominal trajectories and impedances in a structured way. With this library of actions, it would be especially interesting to preform simple Task and Motion Planning (TAMP) applications as discussed in the last few lectures of class. Many of the ideas of dynamic primitives may become clearer after connecting low level control tricks (inspired by humans) to higher level planning questions.

A. *Stability*

Originally, we wanted to try to super impose gripper and joint impedances without the use of a nullspace projector. In addition to ensuring passivity, this approach can move seamlessly into and out of singularities. However, super imposing the gripper and joint impedances directly will always result in a task conflict between gripper and joint space, unless the robot is at the nominal joint position. Interestingly, recent work showed that when the nullspace between task space and joint space is large enough, superimposing impedances can be comparable to nullspace projection [14]. For this reason, this task may be especially interesting as the combined robots have 14 degrees of freedom to control a drill with only 6 (and some of those 6 degrees of freedom are not critical for drilling).

However, in this work we made the choice to use nullspace projection so that the waypoints could be chosen by hand. In our simulation we observed some very slow instability in certain cases. As mentioned in the methods, this is suspected to result from the simulation's relatively long time-step (500-1000 Hz). However, this could have also resulted from the nonpassive nullspace projection, which used a Moore Penrose pseudo inverse.

B. *Building Actions*

After developing this two-arm simulation with the ability to perform both joint and end-effector impedance control, we see some potential for optimization methods to select our impedance parameters and our waypoints and minimum jerk parameters. By using dynamic primitives as the basis for this optimization, the space we are searching in becomes less complicated, perhaps allowing for more consistent minima or maxima to be found

One interesting aspect of the class that stuck out was managing contact at multiple points (e.g., the hugging punyo robot). We believe that this drilling task might be a great example where an optimal control method based on primitives

could find interesting solutions. When humans use a power drill, they frequently make multiple contacts with the environment, often to brace themselves (e.g. pushing against a wall or pushing their elbow against their torso). These actions effectively increase the stiffness at the hand without requiring an increasing muscle activity. Normal robotic control strategies only search for trajectories that avoid collision entirely, so they might miss this specific control solution. However, controlling the iiwa by superimposing joint impedances may allow trajectory optimization to find this type of solution.

V. Conclusions

We set out to simulate the complex task of drilling in both the unimanual and bimanual case. Although the task involves many different types of instabilities, humans are able to accomplish this task with little to no training. We controlled both iiwas by superimposing a joint impedance, gravity compensation, feed forward torque, and an impedance at the gripper. We set chose our impedances to be similar to a human's and used a minimum jerk trajectory moving between waypoints as our nominal position to try to mirror how human control may work. By controlling both iiwas in this way we were able to successfully manipulate the power drill and apply 32 Newtons of force to it to simulate a drilling motion. We saw qualitative differences between the unimanual and bimanual cases, arising from the extra stability in the bimanual case. By simulating all of this in drake, we gained experience and confidence in using drake and see usefulness for it in our research moving forward.

VI. Refrences

[1] D. Rancourt and N. Hogan, "Stability in Force-Production Tasks," *J. Mot. Behav.*, vol. 33, no. 2, pp. 193–204, 2001.

[2] J. E. Colgate and N. Hogan, "Robust control of dynamically interacting systems," *Int. J. Control*, vol. 48, no. 1, pp. 65–88, Jul. 1988.

[3] J. Edward Colgate, "Strictly positive real admittances for coupled stability," *J. Franklin Inst.*, vol. 329, no. 3, pp. 429–444, May 1992.

[4] N. Hogan, "Physical interaction via dynamic primitives," in *Geometric and numerical foundations of movements*, J.-P. Laumond, N. Mansard, and J.-B. Lasserre, Eds. Springer, 2017, pp. 269–299.

[5] N. Hogan and D. Sternad, "Dynamic primitives of motor behavior," *Biol. Cybern.*, vol. 106, no. 11–12, pp. 727–739, Dec. 2012.

[6] N. Hogan, "A General Actuator Model Based on Nonlinear Equivalent Networks," *IEEE/ASME Trans. Mechatronics*, vol. 19, no. 6, pp. 1929–1939, Dec. 2014.

[7] J. Y. S. Luh, R. P. C. Paul, and M. W. Walker, "Resolved-Acceleration Control of Mechanical Manipulators," *IEEE Trans. Automat. Contr.*, vol. 25, no. 3, pp. 468–474, 1980.

[8] C. Natale, *Interaction control of robot manipulators: six degrees-of-freedom tasks*. Springer Science \& Business Media, 2003.

[9] A. Dietrich, C. Ott, and A. Albu-Schäffer, "An overview of null space projections for redundant, torque-controlled robots," *Int. J. Rob. Res.*, vol. 34, no. 11, pp. 1385–1400, Sep. 2015.

[10] O. Khatib, "A unified approach for motion and force control of robot manipulators: The operational space formulation," *IEEE J. Robot. Autom.*, vol. 3, no. 1, pp. 43–53, Feb. 1987.

[11] N. Hogan, "An organizing principle for a class of voluntary movements," *J. Neurosci.*, vol. 4, no. 11, pp. 2745–2754, 1984.

[12] T. Flash, "The control of hand equilibrium trajectories in multi-joint arm movements," *Biol. Cybern.*, vol. 57, no. 4, pp. 257–274, 1987.

[13] P. Marion, P. R. Florence, L. Manuelli, and R. Tedrake, "Label Fusion: A Pipeline for Generating Ground Truth Labels for Real RGBD Data of Cluttered Scenes," *Proc. - IEEE Int. Conf. Robot. Autom.*, pp. 3235–3242, Sep. 2018.

[14] J. Hermus, J. Lachner, D. Verdi, and N. Hogan, "Exploiting Redundancy to Facilitate Physical Interaction," *IEEE Trans. Robot.*, pp. 1–17, 2021.

Github link: https://github.com/nicarons/6_843_Final_Project
Project Video: https://youtu.be/djhSE1Nj9u8

VII. Appendix 1

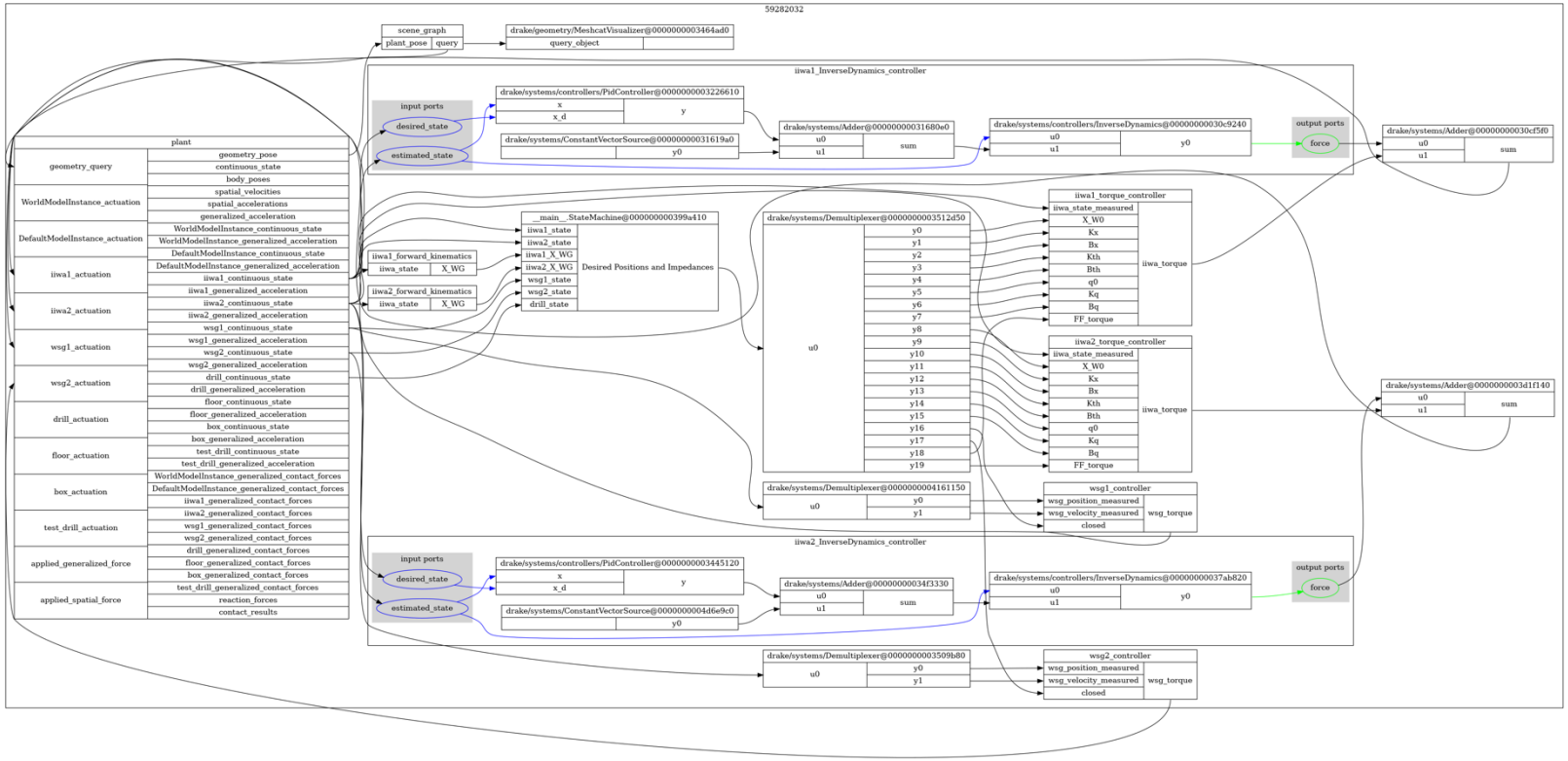

Figure 6: The block diagram for our simulation. The nominal positions and impedances are set by a state machine while our torque controller systems handle the implementation of the torque output.